CHEMISTRY
A EUROPEAN JOURNAL

DOI: 10.1002/chem.201000230

Immunosuppressive Resveratrol Aneuploids from *Hopea chinensis*

Hui Ming Ge,[a] Wen Hao Yang,[a] Yan Shen,[a] Nan Jiang,[b] Zhi Kai Guo,[a] Qiong Luo,[a] Qiang Xu,[a] Jing Ma,[b] and Ren Xiang Tan*[a]

Abstract: Two novel resveratrol aneuploids, hopeachinols A (**1**) and B (**2**), as well as a potent immunosuppressive polyphenol diptoindonesin G (**3**) were characterized from the ethanol extract of *Hopea chinensis* stem barks. The structure of the polyphenols was accommodated by comprehensive spectroscopic analysis with the absolute stereochemistry determined by the CD approach coupled with theoretical ECD spectra computer-generated through the Gaussian 03 program. The distinct structure and biological profile of **3** recommended it as a starting molecule for the relevant drug discovery.

Keywords: *Hopea chinensis* · immunosuppressants · natural products · resveratrol aneuploids · structure elucidation

Introduction

Immunosuppressants are imperative both for organ recipients, and for patients suffering from immune-associated diseases, such as arthritis and asthma.[1] However, most of the immunosuppressive drugs currently available, including glucocorticoids, cyclophosphamide, and even cyclosporine A, have been reported to inevitably possess severe side effects primarily owing to poor selectivity.[2] Therefore, there is an urgent need for new potent immunosuppressive agents with negligible or acceptable toxicity. Recently, some substantially immunosuppressive and less-toxic polyphenols have received increasing chemical and biological attention. (−)-Epigallocatechin-3-*O*-gallate, an anti-inflammatory and immunomodulatory phytochemical rich in green tea, has been a common research topic of many groups.[3] In our state key laboratory, astilbin was characterized from the *Smilax glabra* rhizome as an immunosuppressive flavonoid unique in its selective inhibition on activated T lymphocytes,[4] and dalesconols A and B were identified as novel immunosuppressive polyphenols with higher selectivity.[5] Those findings encouraged us to search for promising immunosuppressants from the *Hopea* species of the Dipterocarpaceae family, which were shown to be abundant in bioactive polyphenols.[6] We hereby wish to report the structure determination and immunosuppressive activity of the three resveratrol aneuploids from stem barks of *Hopea chinensis* endemic to the Hainan Island (China).

[a] Dr. H. M. Ge, W. H. Yang, Dr. Y. Shen, Z. K. Guo, Q. Luo, Prof. Q. Xu, Prof. R. X. Tan
Institute of Functional Biomolecules
State Key Laboratory of Pharmaceutical Biotechnology
School of Lifesciences, Nanjing University
Nanjing 210093 (China)
Fax: (+86) 25-83302728
E-mail: rxtan@nju.edu.cn

[b] Dr. N. Jiang, Prof. J. Ma
Institute of Theoretical and Computational Chemistry
Key Laboratory of Mesoscopic Chemistry of MOE
School of Chemistry and Chemical Engineering
Nanjing University, Nanjing 210093 (China)

Supporting information for this article is available on the WWW under http://dx.doi.org/10.1002/chem.201000230.

Results and Discussion

Hopeachinol A (**1**), an orange amorphous powder, the HRESIMS spectrum of which gave a protonated molecular-ion peak at 587.1338, which indicated that the molecular formula was $C_{35}H_{23}O_9$ (calcd to be 587.1339). The IR spectrum of **1** suggested the coexistence of hydroxyl (3230 cm^{-1}), ketone (1612 cm^{-1}), and aromatic (1585 and 1453 cm^{-1}) groups. The ^1H NMR and COSY sprectra of **1** displayed two coupled aliphatic protons and fourteen aromatic protons including two sets of *ortho*-coupled protons ascrible to two 1,4-disubstituted phenyl rings ($\delta_{H\text{-}2a(6a)}=7.81$ (2H, d, $J=8.5$ Hz), $\delta_{H\text{-}3a(5a)}=7.10$ (2H, d, $J=8.5$ Hz), $\delta_{H\text{-}2b(6b)}=7.24$ (2H, d, $J=8.5$ Hz), and $\delta_{H\text{-}3b(5b)}=6.82$ ppm (2H, d, $J=8.5$ Hz)), one 1,3,5-trisubstituted phenyl ring ($\delta_{H\text{-}10b(14b)}=6.20$ (2H, brs), $\delta_{H\text{-}12b}=6.19$ ppm (1H, brs)), a 1,2,3,5-tetrasubstituted phenyl ring ($\delta_{H\text{-}10a}=7.20$ (brs) and $\delta_{H\text{-}12a}=6.30$ ppm

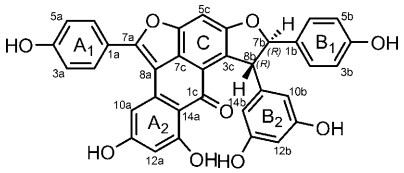

hopeachinol A (**1**)

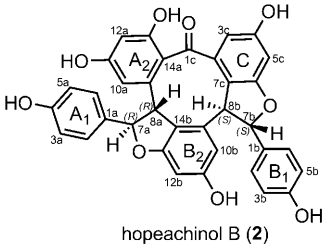

hopeachinol B (**2**)

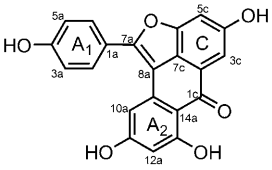

diptoindonesin G (**3**)

(brs)), and a pentasubstited aromatic ring ($\delta_{H\text{-}5c}=7.48$ ppm (1H, s)), as well as an intramolecular hydrogen bond with a proton signal at $\delta=13.98$ ppm. These motifs, together with the elemental composition $C_{35}H_{22}O_9$, suggested that compound **1** may be a sester-resveratrol. The comparison of the ^{13}C NMR spectrum of **1** with that of diptoindonesin G (**3**) indicated that it possessed a substructure sharing the same skeleton with diptoindonesin G (**3**),[7] whereas the remaining motif was a stilbene unit as determined after scrutizing the HMBC correlations between H-8b/C-10b and H-7b/C-2b(5b) (Figure 1, Table 1). The two partial structures were connected by an ether linkage between C-7b/C-4c and a C–C bond between C-8b/C-3c, as evidenced from the distinct HMBC correlations between H-7b/C-4c, H-8b/C-2c, and H-8b/C-4c. Therefore, the planar structure of **1** was constructed as a sester-resveratrol.

The relative configuration of the two chiral carbon atoms (7b/8b) could be unambiguously determined as *trans* by NOE correlations between H-7b/H-10b and H-8b/H-2b(6b) (Figure 1, Table 1).

To assign the absolute stereochemistry of **1**, the electronic circular dichroism (ECD) spectra affordable through quantum-chemical calculations were used.[8] The optimized geometric information for (7b*R*,8b*R*)-**1** are listed in Table S1 (Supporting Information). The calculated ECD spectra of (7b*R*,8b*R*)-**1** and its enantiomer (7b*S*,8b*S*)-**1** after a UV correction of 16 nm (see Figure S1 in the Supporting Information), were depicted in Figure 2. The ECD spectrum gener-

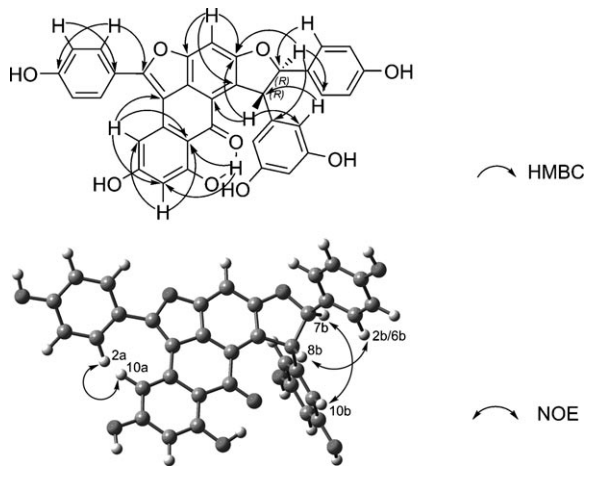

Figure 1. Key HMBC and NOE correlations of **1**. The optimized structural information for **1** within the PCM model (acetone solvent: dielectric constant $\varepsilon=20.70$) at the B3LYP/6-31G(d) level.

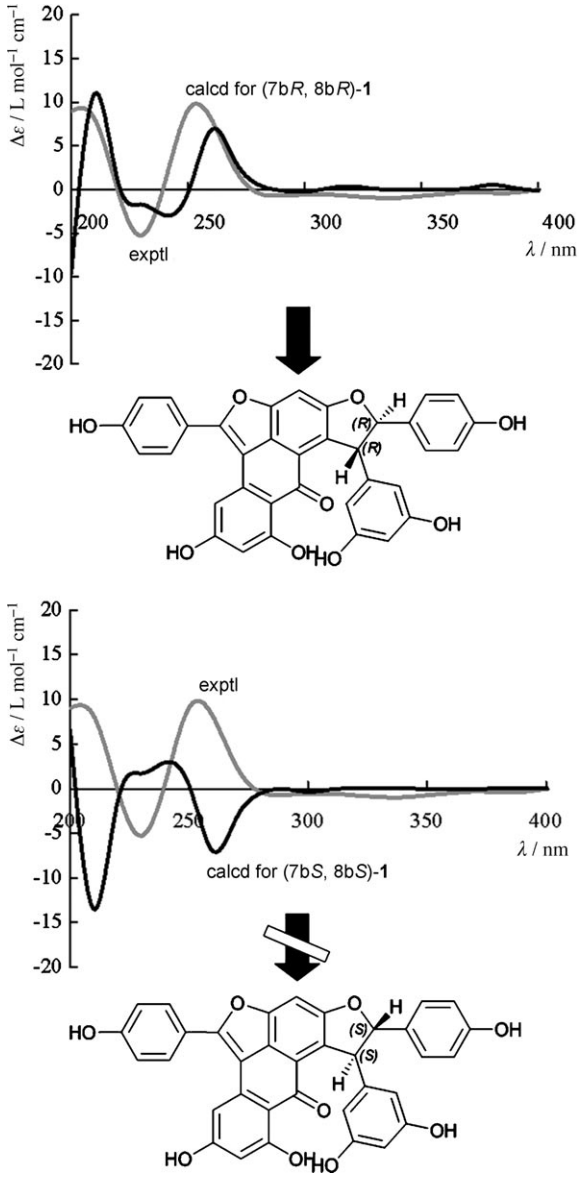

Figure 2. Allocation of the absolute configuration of **1** as 7b*R*,8b*R* by comparison between its experimental (——) and calculated (——, for both enantiomers) ECD spectra.

Table 1. NMR spectroscopic data of compounds **1** and **2**.[a]

No.	Hopeachinol A (**1**)				Hopeachinol B (**2**)			
	δ_C[b]	δ_H (mult., J)[b]	HMBC (H→C)	NOESY[c]	δ_C[b]	δ_H (mult., J)[b]	HMBC (H→C)	NOESY[c]
1a	122.5				131.8			
2a/6a	131.6	7.81 (d, 8.2)	4a, 7a, 6a/2a	3a/5a, 10a	128.6	7.16 (d, 8.5)	4a, 7a, 6a/2a	3a/5a, 7a, 8a
3a/5a	117.0	7.10 (d, 8.2)	1a, 5a/3a, 4a	2a/6a	116.0	6.78 (d, 8.5)	1a, 5a/3a, 4a	2a/6a
4a	160.6				158.5			
7a	157.6				90.6	5.88 (d, 8.0)	1a, 2a/6a, 9a, 13b, 14b	2a/6a, 10a > 8a
8a	109.7				51.2	4.81 (d, 8.0)	1a, 10a, 14a, 9b,13b, 14b, 7a, 9a	2a/6a > 7a
9a	135.6				143.7			
10a	103.6	7.20 (s)	8a, 12a, 14a	2a/6a	105.8	6.63 (d, 1.7)	8a, 12a, 14a, 11a	7a
11a	164.6				162.9			
12a	103.1	6.30 (s)	10a, 14a, 11a, 13a		102.8	6.33 (d, 1.7)	10a, 14a, 11a, 13a	
13a	167.9	14.0 (brs, -OH)	12a, 13a, 14a		160.6	10.6 (br s, -OH)		
14a	112.4				119.2			
1b	133.8				132.1			
2b/6b	127.7	7.24 (d, 8.2)	4b, 7b, 6b/2b	3b/5b, 7b, 8b	128.4	7.07 (d, 8.5)	4b, 7b, 6b/2b	3b/5b, 7b, 8b
3b/5b	116.3	6.82 (d, 8.2)	1b, 5b/3b, 4b	2b/6b	116.1	6.71 (d, 8.5)	1b, 5b/3b, 4b	2b/6b
4b	158.4				158.3			
7b	94.9	5.68 (d, 2.8)	2b/6b, 4c, 9b	2b/6b, 10b/14b > 8b	89.0	6.05 (s)	1b, 2b/6b, 9b, 6c, 7c	2b/6b, 8b, 10b
8b	56.7	4.98 (d, 2.8)	1b, 10b/14b, 4c, 9b, 3c	2b/6b, 10b/14b > 7b	48.3	4.16 (s)	1b, 10b, 14b, 2c, 6c	2b/6b, 7b, 10b
9b	147.2				139.5			
10b	106.8	6.20 (s)	8b, 12b, 11b/13b	7b, 8b	106.6	6.68 (d, 1.1)	8b, 12b, 14b, 11b	7b, 8b
11b	159.5				159.9			
12b	102.0	6.19 (s)	10b/14b, 11b/13b		97.2	6.27 (d, 1.1)	10b, 14b, 11b, 13b	
13b	159.5				161.3			
14b	106.8	6.20 (s)	8b, 12b, 11b/13b	7b, 8b	121.7			
1c	187.5				197.7			
2c	126.3				139.4			
3c	126.7				107.1	6.85 (d, 1.7)	1c, 5c, 7c, 4c	
4c	161.6				159.8			
5c	99.3	7.48 (s)	3c, 4c, 6c		102.9	6.51 (d, 1.7)	3c, 7c, 4c, 6c	
6c	153.8				160.6			
7c	121.7				121.3			

[a] Data were recorded in [D6]acetone at 500 MHz for ^{1}H and 2D NMR, and 125 MHz for ^{13}C NMR spectra. [b] δ in ppm, J in Hz. [c] The sign > differentiates strong and weak correlations.

ated for (7b*R*,8b*R*)-**1** showing the positive (208 and 264 nm) and negative (223 and 244 nm) Cotton effects (CE) was in good agreement with the experimental data of **1**, whereas the calculated ECD spectrum for (7b*S*,8b*S*)-**1** was almost opposite to the experimental curve. The excitations from π-type molecular orbitals (MO) to π*-type MO of aromatic rings played a dominant role in the absorbed bands (see Figure 3 and Table S2 in the Supporting Information). The electronic transitions of MO150→MO157 ($\pi_{C=C}\rightarrow\pi^*_{C=C}$) and MO144→MO153 ($\pi_{C=C}\rightarrow\pi^*_{C=O}$) contributed to the positive rotatory strengths at 208 and 264 nm, respectively. They were associated with the experimental CE at 210 and 253 nm (see Table S1 and Figure S2 in the Supporting Information). The calculated negative CE at 223 and 244 nm could be assigned to the broad band at about 227 nm in the experimental ECD spectrum, representing the excitations of

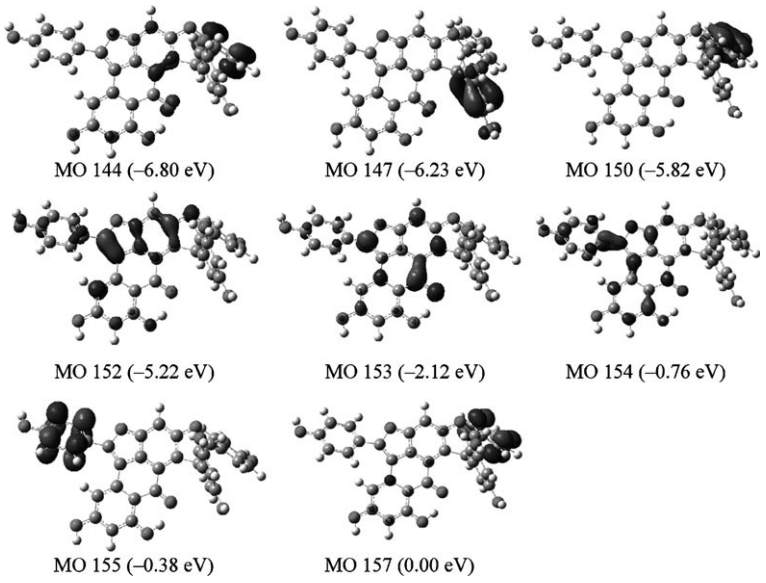

Figure 3. The most important orbitals of the optimized conformer of compound (7b*R*,8b*R*)-**1**. The optimized conformation is obtained at the B3LYP/6-31G(d) level in the PCM (MeOH solvent: dielectric constant $\varepsilon = 32.63$) model.

MO147→MO154 ($\pi_{C=C}\rightarrow\pi^*_{C=O}$) and MO152→MO155 ($\pi_{C=C}\rightarrow\pi^*_{C=C}$).

Hopeachinol B (**2**) was isolated as a yellowish amorphous powder, the HRESIMS spectrum of which gave a protonated molecular-ion peak at *m/z*: 589.1496, which indicated that the molecular formula was $C_{35}H_{24}O_9$ ($[M+H]^+$ calcd for 589.1493) with 24 degrees of unsaturation. The IR spectrum of **2** also suggested the presence of hydroxyl (3263 cm^{-1}), ketone (1613 cm^{-1}), and aromatic (1594 and 1437 cm^{-1}) functionalities. These all indicated that hopeachinol B could be another sester-resveratrol. The ^1H NMR and COSY spectra of **2** acquired in [D_6]acetone displayed two sets of coupled aliphatic protons ($\delta_{H\text{-}8a}=4.81$ (1H, d, $J=8.0$ Hz) and $\delta_{H\text{-}7a}=5.88$ ppm (1H, d, $J=8.0$ Hz); $\delta_{H\text{-}8b}=4.16$ (1H, brs) and $\delta_{H\text{-}7b}=6.05$ ppm (1H, brs)), ten aromatic protons including two sets of *ortho*-coupled protons assignable to a 1,4-disubstituted phenyl ring ($\delta_{H\text{-}3a(5a)}=6.78$ (2H, d, $J=8.5$ Hz) and $\delta_{H\text{-}2a(6a)}=7.16$ ppm (2H, d, $J=8.5$ Hz); $\delta=6.71_{H\text{-}3a(5a)}$ (2H, d, $J=8.5$ Hz) and $\delta_{H\text{-}2a(6a)}=7.07$ ppm (2H, d, $J=8.5$ Hz)), three sets of *meta*-coupled protons on three 1,2,3,5-tetrasubstituted phenyl rings ($\delta_{H\text{-}12b}=6.27$ (1H, d, $J=1.1$ Hz) and $\delta_{H\text{-}10b}=6.68$ ppm (1H, d, $J=1.1$ Hz); $\delta_{H\text{-}12a}=6.33$ (1H, d, $J=1.7$ Hz) and $\delta_{H\text{-}10a}=6.63$ ppm (1H, d, $J=1.7$ Hz); $\delta_{H\text{-}3c}=6.85$ (1H, d, $J=1.7$ Hz) and $\delta_{H\text{-}5c}=6.51$ ppm (1H, d, $J=1.7$ Hz)), and an intramolecular hydrogen bond with a proton signal at $\delta=10.55$ ppm. The HMBC correlations of H-2a(6a)/C-7a, H-8a/C-1a, H-7a/C-9a, and H-10a/C-8a (Figure 4, Table 1) suggested a substructure of a stilbene skeleton (ring A_1–C-7a–C-8a—ring A_2). The HMBC correlations of H-2b(6b)/C-7b, H-8b/C-1b, H-7b/C-9b, and H-10b/C-8b indicated another stilbene skeleton (ring B_1–C-7b–C-8b—ring B_2). The HMBC correlations H-3c/C-1c indicated the presence of an acetophenonyl moiety. Subtracting 21 degrees of unsaturation (five phenyl rings and a carbonyl), compound **2** had three more rings. Two oxygenated carbon atoms C-7a and C-7b resonated at $\delta=90.6$ and 89.0 ppm in its ^{13}C NMR spectra, respectively, together with HMBC correlations of H-7a/C-13b, H-8a/C-9b, H-7b/C-6c, and H-8b/C-2c, which revealed the presence of two dihydrofuran rings. The presence of an intramolecular hydrogen bond formed by the carbonyl at C-1c and hydroxyl at C-14a revealed that C-1b and C-14a were linked directly to form the last required big rings. Thus, the planar structure of hopeachinol B (**2**) was determined (see graphic).

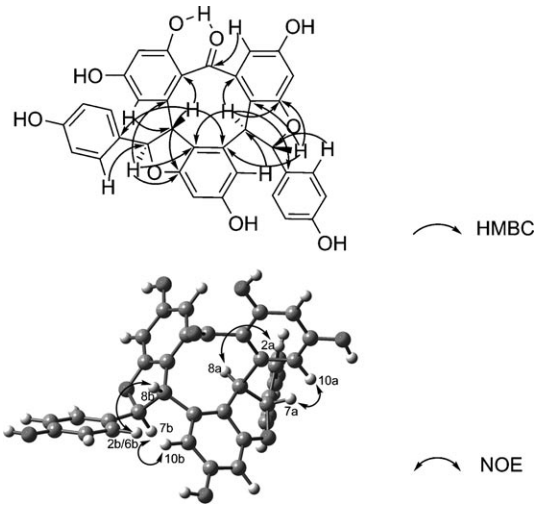

Figure 4. Key HMBC and NOE correlations of **2**. The optimized structural information for **2** within the PCM model (acetone solvent: dielectric constant $\varepsilon=20.70$) at the B3LYP/6-31G(d) level.

The relative configuration of hopeachinol B was determined unambiguously by NOESY correlations (Figure 4, Table 1). The NOEs for H-7a/H-10a, H-8a/H-2a(6a), H-7b/H-10b, and H-8b/H-2b(6b) indicated *trans* configurations for H-7a/H-8a and H-7b/H-8b. However, no NOE correlation was detected for H-8a/H-8b, which suggested a *trans* configuration for H-8a/H-8b.[9] Thus, the relative configuration of **2** was established.

A comparison was also made between the experimental CD and calculated ECD spectra for (7a*R*,8a*R*,7b*S*,8b*S*)-**2** and (7a*S*,8a*S*,7b*R*,8b*R*)-**2** after a UV correction of 16 nm (Figure 5 and Figure S2 in the Supporting Information). The coordinate information of (7a*R*,8a*R*,7b*S*,8b*S*)-**2** was given in Table S3 (Supporting Information). As shown in Figure 5, the calculated ECD curve for (7a*R*,8a*R*,7b*S*,8b*S*)-**2** agreed well with the experimental ECD spectrum, which was opposite to that calculated for (7a*S*,8a*S*,7b*R*,8b*R*)-**2**. The calculated negative Cotton effects at 224 and 284 nm could be assigned to the bands at 225 and 279 nm in the experimental ECD spectrum. As shown in Figure 6 and Table S4 (Supporting Information), the transitions from π-type (filled C=C orbital) and n-type (lone pair orbital on oxygen) to π*-type (antibonding C=C and C=O orbitals) molecular orbitals (MO), MO 142→154 and MO 153→155, contributed to these absorption bands. In the experimental ECD spectrum, two positive bands were observed at 211 and 242 nm, which were well reproduced by the calculations (204 and 237 nm, respectively). The $\pi\rightarrow\pi^*$ and $n\rightarrow\pi^*$ excitations (MO 145→160, MO 149→161, and MO 151→162) played a dominant role. In addition, a positive Cotton effect at 302 nm, arising from $\pi_{C=C}\rightarrow\pi^*_{C=C}$ excitation (MO 148→154), is produced by our calculations.

Compound **3** was isolated as a red amorphous powder. Its structure was identified as diptoindonesin G by comparing its MS and NMR spectroscopic data with literature.[7]

The resveratrol aneuploids **1**–**3** were tested for immunosuppresive activity by using a Con A induced proliferation of mouse splenic lymphocytes (T cells) assay. Resveratrol and a clinically prescribed immunosuppressant cyclosporin A were used as controls. Compound **3** was found to be significantly active with an IC_{50} value of 10.8 μM, approximately 16-fold higher inhibitory activity than resveratrol ($IC_{50}=170.6$ μM), whereas hopeachinols A (**1**) and B (**2**) exhibited weak and moderate activity with IC_{50} values of >100 and 50.1 μM, respectively. As shown in Figure 7B, compound **3** suppressed Con A induced cell proliferation by 60% at 15 μM at which the survival of normal splenic cells was slightly influenced (Figure 7A), which suggested that the inhibition of compound **3** is not from the aspect of cytotoxity.

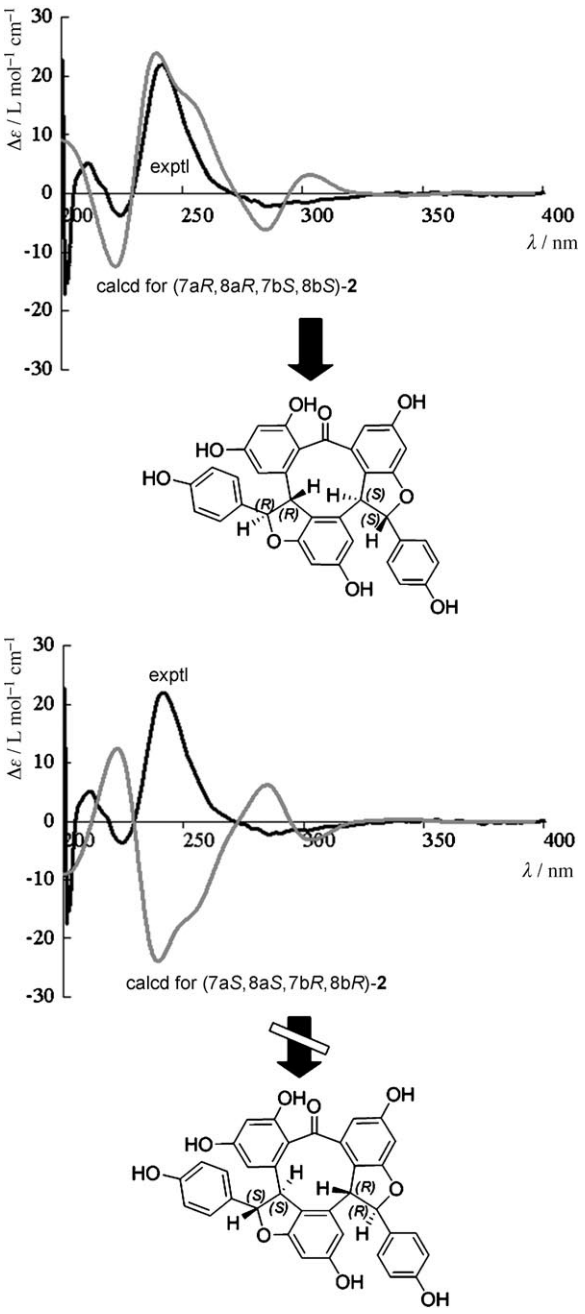

Figure 5. Assignment of the absolute configuration of **2** as 7a*R*,8a*R*,7b*S*,8b*S* by comparison between its experimental (——) and calculated (——, for both enantiomers) ECD spectra.

Interestingly, compound **3** contained an 8-hydroxynaphthalen-1(4*H*)one scaffold, which happens to be well comparable to 5-hydroxychroman-4-one and 8-hydroxy-3,4-dihydronaphthalen-1(2*H*)one moieties structured in other immunosuppressive natural products astilbin[4] and dalesconols,[5] respectively, with their bioactivity being all recognized by the activated T-lymphocyte assay in our state key laboratory. However, it was noteworthy that compound **1**, though containing a 5-hydroxychroman-4-one moiety, possessed negligible immunosuppressive activity presumably because the scaffold could have been "masked" by the phenyl group in its neighbourhood.

Furthermore, the effects of compound **3** on the apoptosis of Con A activated T cells were investigated by PI and annexin V double staining. The percentage of apoptotic activated T cells was increased dose-dependently by compound **3**, 15 μM of which displayed comparable activity to 50 μM quercetin, a positive control (Figure 8A). When the apoptotic signaling pathway was examined by western blotting, cleaved caspase-3, 7, 9, and PARP were observed to appear more intensively in **3**-treated activated T cells (Figure 8B). Therefore, the immunosuppressive activity of compound **3** is possibly due to its induction of apoptosis in activated T cells.

Conclusion

To the best of our knowledge, only very few natural resveratrol aneuploids have been characterized previously.[7,10] Herein, two structurally unusual and one biologically promising resvertrol aneuploid were isolated from a tropical Dipterocarpaceae plant *Hopea chinensis*. The structures were determined by comprehensive spectroscopic data coupled with the computational quantum-chemical method. The ECD spectrum supplied a valid method for determining the absolute configurations for oligostilbenoids, most of which were still obscure.[6,10] The difference in the bioactivity of the resveratrol aneuploids highlighted that a readily accessible 8-hydroxynaphthalen-1(4*H*)one moiety and its isostere-alike residues 5-hydroxychroman-4-one seemed to be essential for some immunosuppressive natural products.[4,5] Finally, the unique architecture, potent immunosuppresive activity, and lower toxicity of compound **3** suggested collectively that it could be a favorable starting molecule for the immunosuppressive drug discovery.

Experimental Section

General reagents and instrumentation: Optical rotations were recorded on a Rudolph Research Analytical Autopol III automatic polarimeter. The UV spectrum was recorded on a Hitachi U-3000 spectrophotometer. CD spectra were obtained on a JASCO J-810 spectrometer, and the IR spectrum was measured on a Nexus 870 FTIR spectrometer. HRESIMS spectra were recorded on an Agilent 6210 TOF LCMS equipped with an electrospray ionization (ESI) probe operating in positive-ion mode with direct infusion; NMR spectroscopic data were acquired in [D6]acetone on a Bruker DRX500 NMR spectrometer with tetramethylsilane (TMS) and solvent signals as internal references. Silica gel (200–300 mesh) for column chromatography was produced by Qingdao Marine Chemical Factory, Qingdao (China). Sephadex LH-20 was purchased from Pharmacia Biotech (Sweden). HPLC analysis was performed by using a 250 × 10 mm, 5 μm, Hypersil ODS column (Thermo Fisher Scientific, USA) on a Hitachi HPLC system consisting of a L-7110 pump (Hitachi) and a L-7400 UV/Vis Detector (Hitachi). [D_6]acetone used for NMR spectroscopic measurements was purchased from Merck. All chemicals used in the study were of analytical grade.

Plant material: The stems and twigs of *Hopea chinensis* were collected in August 2008 from the Botanical Garden at Jianfeng Town, Ledong

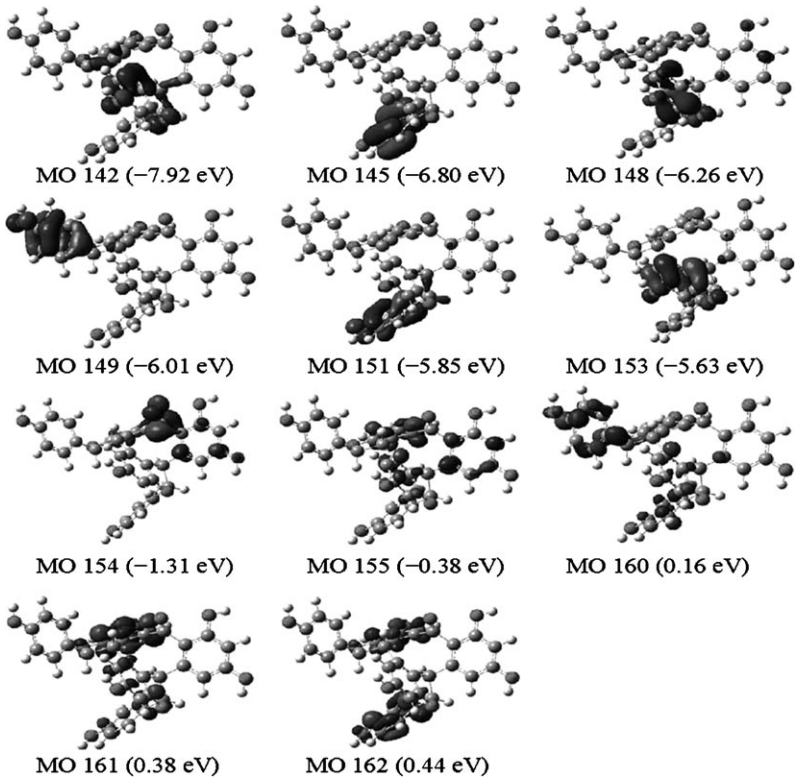

Figure 6. The most important orbitals of the optimized conformer of compound (7a*R*,8a*R*,7b*S*,8b*S*)-**2**. The optimized conformation is obtained at the B3LYP/6-31G(d) level in the PCM (MeOH solvent: dielectric constant $\varepsilon=$ 32.63) model.

County, Hainan Island (China). A voucher specimen (no. IFB-20080820) was preserved at the Institute of Functional Biomolecules, Nanjing University. The specimen was identified by Prof. X. J. Tian (Nanjing University, Nanjing, China).

Extraction and isolation procedures: The air-dried and powdered stem woods of *Hopea chinensis* (16.5 kg) were extracted with EtOH (3×20 L) at room temperature and concentrated in vacuo to give a crude extract (121.9 g), which was subsequently diluted with H_2O (500 mL) to give an aqueous suspension. After defatting by partitioning with petroleum ether (3×500 mL), the suspension was extracted with EtOAc (3×500 mL). The EtOAc extract (82 g) was chromatographed on a silica-gel column eluted with mixtures of $CHCl_3$/MeOH (100:0, 100:5, 100:10, 100:15, 100:20, 100:30, 100:40, 100:60, and 0:100, v/v, each 3.5 L) to give a total of 33 fractions. Fractions of similar compositions, as determined by TLC, were pooled, resulting in eight fractions (A–H). Fraction C (3.5 g) was subjected to passage over a second silica-gel column, eluting with $CHCl_3$/MeOH increasing in polarity (100:5–100:20), to give six subfractions (C1-C6). Fraction C1 (98 mg) was purified by using Sephadex LH-20 eluted with $CHCl_3$/MeOH (1:1) to afford compound **1** (8 mg) and a mixture, which was further purified by a silica-gel column eluting with $CHCl_3$/MeOH (100:10) to give compound **3** (4 mg). Fraction D (6.0 g) was chromatographed on a Sephadex LH-20 column by elution with MeOH to give 13 subfractions (D1–D13). Fraction D9 was purified by HPLC (MeOH/H_2O 53:47) to give compound **2** (8 mg, $t_R=10.6$ min).

Computational details: The theoretical calculation of the ECD spectrum was performed with the Gaussian 03 program.[8a] Firstly, the geometric optimizations of the studied systems in CH_3OH solvent are carried out by using density-functional theory (DFT) at the B3LYP/6-31G(d) level. The effects of solvent on the electronic structures of the solutes were simulated with the self-consistent reaction field (SCRF) method within the framework of polarizable continuum model (PCM). The dielectric constant, ε, with value of 32.63 for CH_3OH is employed. Then, on the basis of the optimized geometries, the excited-state calculations were performed. The spin-allowed excitation energies and rotatory strengths of the lowest 120 excited states have been calculated by a combination of time-dependent DFT with the PCM model (TD-DFT/PCM) with the 6-31G(d) basis set. The final ECD spectra were produced according to Equation (1), in which $\Delta\varepsilon_n$ is the peak intensity in the unit of $L\,mol^{-1}\,cm^{-1}$, λ_n is the wavelength of the nth transition, and $\Delta\lambda_n$ is the half-width at 1/e of the peak maximum, and Equation (2) in which the half-width $\Delta\lambda_n=\lambda_n^2\Delta\tilde{\nu}$ with $\Delta\tilde{\nu}=1200\,cm^{-1}$ and R_n is the rotatory strength given in 10^{-40} cgs:[11]

$$\Delta\varepsilon(\lambda)=\sum_n \Delta\varepsilon_n \exp\left[-\left(\frac{\lambda-\lambda_n}{\Delta\lambda_n}\right)^2\right] \quad (1)$$

$$\Delta\varepsilon_n=\frac{\lambda_n R_n}{22.94\sqrt{\pi}\Delta\lambda_n}\times 10^{40} \quad (2)$$

The UV correction, comparison of the predicted overall UV spectrum with the experimentally measured one, is important to assign the absolute configuration from ECD calculations. The systematic errors in the prediction of the wavelength and excited-state ener-

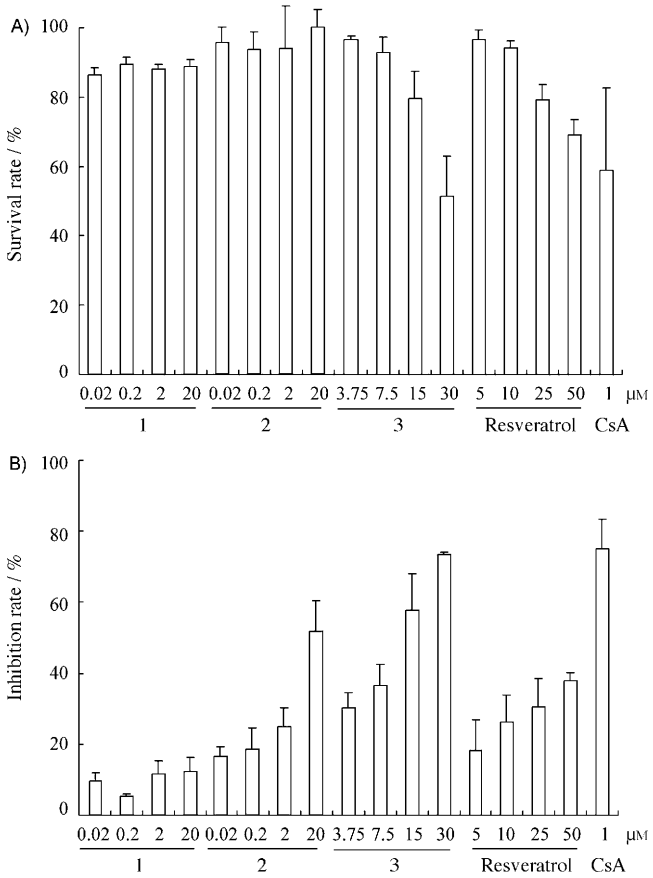

Figure 7. Cytotoxic (A) and immunosuppressive (B) effects of compounds **1**–**3** on mouse splenic cells.

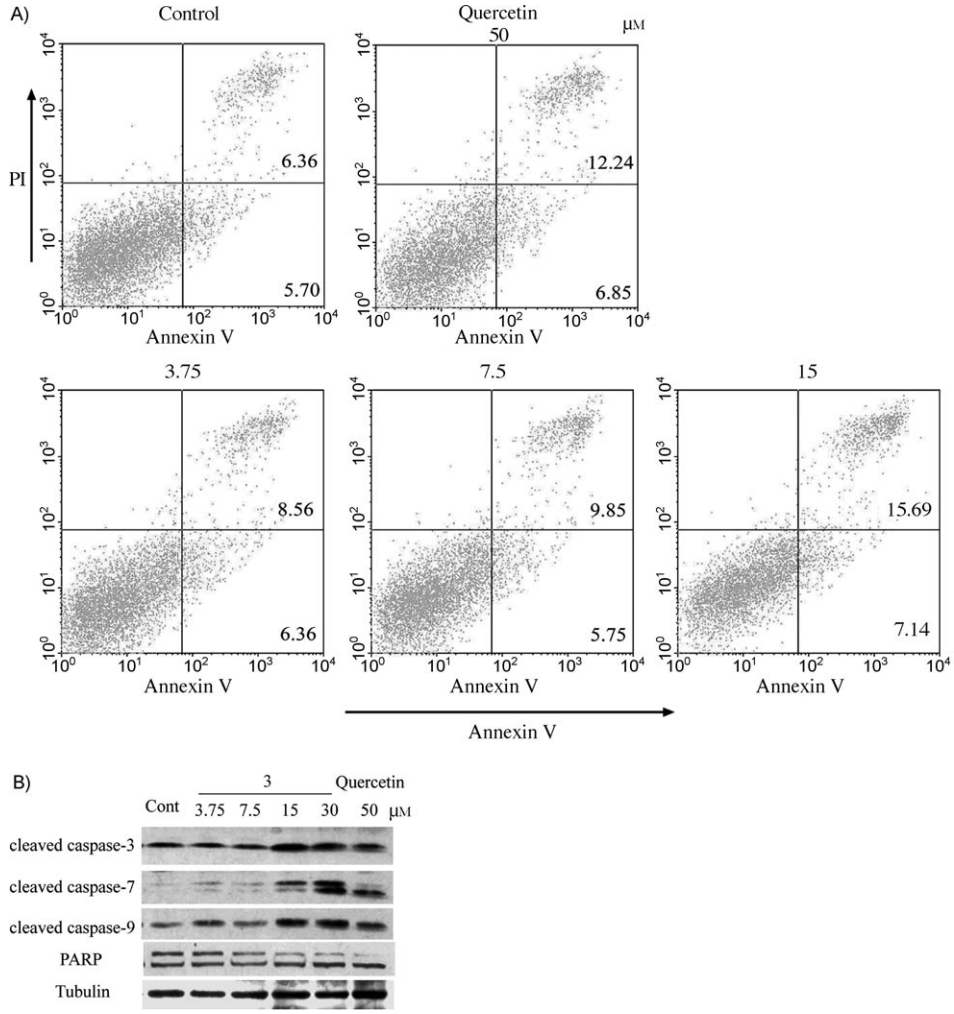

Figure 8. Compound **3**-induced apoptosis of activated T cells. Freshly isolated lymph node cells were activated by Con A for 24 h, and then incubated in the presence of compound **3** or quercetin for a further 24 h. A) PI-annexin V staining. B) Western Blot analysis.

gies are eliminated by adjusting the calculated overall ECD spectrum by the same shift.[12]

Measurement of cell proliferation: Spleen cells isolated from Balb/c mice were seeded in 96 well-plates at a density of 3×10^5 cells per well and activated by Con A (5 μg mL^{-1}) in the presence or absence of various concentrations of compounds for 72 h. 20 μL of MTT (Sigma, MO; 4 mg mL^{-1} in PBS) were added per well 4 h before the end of the incubation. MTT formazan production was dissolved by dimethyl sulfoxide replacing the medium. The optical density at 540 nm (OD_{540}) was measured by a microplate reader. The IC_{50} value was calculated from the correlation curve between the compound concentration and the OD_{540}.

Measurement of apoptotic activated T cells: Lymph node cells isolated from Balb/c mice were activated by Con A (5 μg mL^{-1}) for 24 h, which were indicated as activated cells. The cells were further incubated in the presence or absence of various concentrations of compounds at a density of 5×10^5 cells per well for 24 h. Then the cells were measured by flow cytometry after addition of PI and FITC-conjugated annexin V (Bender, Germany), as preciously described.[13] Samples were analyzed by flow cytometry on a FACScan (Becton Dickinson).

Western blot analysis: In brief, cells were washed with phosphate-buffered saline and lysed in the lysis buffer containing 50 mM TrisCl, 150 mM NaCl, 1% NP40, 100 μg mL^{-1} PMSF. After 10,000×g centrifugation for 10 min, the protein content of the supernatant was determined by a BCA protein assay Kit (Pierce, Rochford, IL). The protein lysates were separated by 10% SDS-PAGE and subsequently electrotransferred onto a polyvinylidene difluoride membrane (Millipore Corp., Bedford, MA). The membrane was blocked with 5% nonfat milk for 2 h at room temperature. The blocked membrane was incubated with the indicated antibodies. Primary antibodies used were against cleaved caspase-3, 7, 9, PARP (Cell Signaling Technology, Beverly, MA) and tubulin (Santa Cruz Biotechnologies, Santa Cruz, CA), and the secondary antibodies were horseradish peroxidise, conjugated goat antimouse, or antirabbit immunoglobulin (Gaithersburg, MD). Protein bands were visualized by using a Western blotting detection system according to the manufacturer's instructions (Cell Signaling Technology).

Hopeachinol A (***1***): Orange amorphous powder; m.p. carbonized over 250 °C; $[\alpha]_D^{24}=-22.4$ ($c=0.107$ in MeOH); for 1D and 2D NMR data, see Table 1 and the Supporting Information; IR (KBr): $\tilde{\nu}=3230$, 2918, 2850, 1612, 1585, 1512, 1453, 1407, 1336, 1270, 1244, 1221, 1170, 1112, 1063, 1042, 998, 834 cm^{-1}; UV/Vis (MeOH): λ_{max} (log ε) = 208 (4.9), 255 (4.5), 364 (4.2), 458 nm (4.1); CD ($c=5.5\times10^{-6}$ g mL^{-1}, MeOH): λ_{max} ($\Delta\varepsilon$) = 211 (+10.5), 230 (−7.7), 252 (+11.7), 339 nm (−1.1); HRESIMS (positive): *m*/*z*: calcd: 587.1337 $[C_{35}H_{23}O_9]^+$; found: 587.1339 $[M+H]^+$.

Hopeachinol B (***2***): Yellowish amorphous powder; m.p. 232–233 °C; $[\alpha]_D^{22}=+37.5$ ($c=0.063$ in MeOH); for 1D and 2D NMR data, see Table 1 and the Supporting Information; IR (KBr): $\tilde{\nu}=3263$, 2958, 2926, 1613, 1594, 1515, 1437, 1362, 1336, 1215, 1171, 1113, 1000, 832 cm^{-1}; UV/Vis (MeOH): λ_{max} (log ε) = 205 (5.9), 281 (5.1), 330 nm (4.7); CD ($c=1\times10^{-5}$ g mL^{-1}, MeOH): λ_{max} ($\Delta\varepsilon$) = 211 (+5.1), 224 (−3.8), 242 (+21.8), 286 nm (−2.2); HRESIMS (positive): *m*/*z*: calcd: 611.1316 $[C_{35}H_{24}Na\ O_9]^+$, 589.1493 $[C_{35}H_{25}O_9]^+$; found: 611.1313 $[M+Na]^+$, 589.1496 $[M+H]^+$.

Acknowledgements

The work was co-supported by grants from the Natural Scientific Foundation of China (20802035 and 30821006), Jiangsu Natural Scientific Foundation (BK2008270), Ministry of Education (200802841022), and Key Projects in the National Science & Technology Pillar Program of China (2009ZX09501-013 and 2009ZX09102-129).

[1] P. F. Halloran, *New Engl. J. Med.* **2004**, *351*, 2715–2729.
[2] a) B. D. Kahan, *Nat. Rev. Immunol.* **2003**, *3*, 831–838; b) H. Hackstein, A. W. Thomson, *Nat. Rev. Immunol.* **2004**, *4*, 24–34.
[3] a) K. Kawai, N. H. Tsuno, J. Kitayama, Y. Okaji, K. Yazawa, M. Asakage, S. Sasaki, T. Watanabe, K. Takahashi, H. Nagawa, *J. Aller-*

gy Clin. Immunol. **2005**, *115*, 186–191; b) S. H. Hyon, D. H. Kim, W. Cui, K. Matsumura, J. Y. Kim, S. Tsutsumi, *Cell Transplant.* **2006**, *15*, 881–883.

[4] M. J. Fei, X. F. Wu, Q. Xu, *J. Allergy Clin. Immunol.* **2005**, *116*, 1350–1356.

[5] Y. L. Zhang, H. M. Ge, W. Zhao, H. Dong, Q. Xu, S. H. Li, J. Li, J. Zhang, Y. C. Song, R. X. Tan. *Angew. Chem.* **2008**, *120, 5907–5910; Angew. Chem. Int. Ed.* **2008**, 47, 5823–5826; *Angew. Chem. Int. Ed.* **2008**, *47*, 5823–5826.

[6] a) H. M. Ge, W. H. Yang, J. Zhang, R. X. Tan, *J. Agric. Food Chem.* **2009**, *57*, 5756–5761; b) H. M. Ge, C. H. Zhu, D. H. Shi, L. D. Zhang, D. Q. Xie, J. Zhang, S. W. Ng, R. X. Tan, *Chem. Eur. J.* **2008**, *14*, 376–381; c) H. M. Ge, B. Huang, S. H. Tan, D. H. Shi, Y. C. Song, R. X. Tan, *J. Nat. Prod.* **2006**, *69*, 1800–1802; d) H. M. Ge, C. Xu, X. T. Wang, B. Huang, R. X. Tan, *Eur. J. Org. Chem.* **2006**, 5551–5554; e) J. Y. Liu, Y. H. Ye, L. Wang, D. H. Shi, R. X. Tan, *Helv. Chim. Acta* **2005**, *88*, 2910–2917.

[7] L. D. Juliawaty, H. Sahidin, H. Euis, S. A. Achmad, Y. M. Syah, J. Latip, I. M. Said, *Nat. Prod. Commun.* **2009**, *4*, 947–950.

[8] a) Gaussian 03, Revision D. 01, M. J. Frisch, G. W. Trucks, H. B. Schlegel, G. E. Scuseria, M. A. Robb, J. R. Cheeseman, J. A. Montgomery, Jr., T. Vreven, K. N. Kudin, J. C. Burant, J. M. Millam, S. S. Iyengar, J. Tomasi, V. Barone, B. Mennucci, M. Cossi, G. Scalmani, N. Rega, G. A. Petersson, H. Nakatsuji, M. Hada, M. Ehara, K. Toyota, R. Fukuda, J. Hasegawa, M. Ishida, T. Nakajima, Y. Honda, O. Kitao, H. Nakai, M. Klene, X. Li, J. E. Knox, H. P. Hratchian, J. B. Cross, V. Bakken, C. Adamo, J. Jaramillo, R. Gomperts, R. E. Stratmann, O. Yazyev, A. J. Austin, R. Cammi, C. Pomelli, J. W. Ochterski, P. Y. Ayala, K. Morokuma, G. A. Voth, P. Salvador, J. J. Dannenberg, V. G. Zakrzewski, S. Dapprich, A. D. Daniels, M. C. Strain, O. Farkas, D. K. Malick, A. D. Rabuck, K. Raghavachari, J. B. Foresman, J. V. Ortiz, Q. Cui, A. G. Baboul, S. Clifford, J. Cioslowski, B. B. Stefanov, G. Liu, A. Liashenko, P. Piskorz, I. Komaromi, R. L. Martin, D. J. Fox, T. Keith, M. A. Al-Laham, C. Y. Peng, A. Nanayakkara, M. Challacombe, P. M. W. Gill, B. Johnson, W. Chen, M. W. Wong, C. Gonzalez, J. A. Pople, Gaussian, Inc., Wallingford, CT, **2004**; b) P. J. Stephens, D. M. McCann, F. J. Devlin, J. R. Cheeseman, M. J. Frisch, *J. Am. Chem. Soc.* **2004**, *126*, 7514–7521; c) P. J. Stephens, D. M. McCann, E. Butkus, S. Stoncius, J. R. Cheeseman, M. J. Frisch, *J. Org. Chem.* **2004**, *69*, 1948–1958; d) D. M. McCann, P. J. Stephens, *J. Org. Chem.* **2006**, *71*, 6074–6098.

[9] a) H. X. Liu, W. H. Lin, J. S. Yang, *Chem. Pharm. Bull.* **2004**, *52*, 1339–1341; b) E. K. Seo, H. Chai, H. L. Constant, T. Santisuk, C. Reutrakul, C. W. W. Beecher, N. R. Farnsworth, G. A. Cordell, J. M. Pezzuto, A. D. Kinghor, *J. Org. Chem.* **1999**, *64*, 6976–6983.

[10] a) T. Tanaka, T. Ito, Y. Ido, T.-K. Son, K. Nakaya, M. Iinuma, M. Ohyama, V. Chelladurai, *Phytochemistry* **2000**, *53*, 1015–1019; b) T. Ito, T. Tanaka, M. Iinuma, K.-i. Nakaya, Y. Takahashi, R. Sawa, J. Murata, D. Darnaedi, *J. Nat. Prod.* **2004**, *67*, 932–937; c) S. G. Wang, D. Y. Ma, C. Q. Hu, *Helv. Chim. Acta* **2005**, *88*, 2315–2321.

[11] A. Jiemchooroj, P. Norman, *J. Chem. Phys.* **2007**, *126*, 134102/1–7.

[12] a) G. Bringmann, S. Busemann in *Natural Product Analysis: Chromatography, Spectroscopy, Biological Testing* (Eds.: P. Schreier, M. Herderich, H.-U. Humpf, W. Schwab), Vieweg, Wiesbaden, **1998**, pp. 195–211; b) G. Bringmann, T. Bruhn, K. Maksimenka, Y. Hemberger, *Eur. J. Org. Chem.* **2009**, 2717–2727.

[13] F. Y. Gong, Y. Shen, C. F. Zhang, J. L. Xu, X. F. Wu, Z. C. Hua, Q. Xu, *Exp. Biol. Med.* **2008**, *233*, 1124–1132.

Received: January 27, 2010

Please note: Minor changes have been made to this manuscript since its publication in *Chemistry–A European Journal* Early View. The Editor.

Published online: April 21, 2010

